PHYSICAL REVIEW A **72**, 042705 (2005)

Total cross-section measurements for positrons and electrons colliding with alkane molecules: Normal hexane and cyclohexane

O. Sueoka, C. Makochekanwa,* H. Tanino, and M. Kimura†
Faculty of Engineering, Yamaguchi University, Tokiwadai 2-16-1, Ube, Yamaguchi 755-8611, Japan
(Received 12 March 2005; published 11 October 2005)

Total cross sections (TCSs) for 0.2–1000 eV positrons and 0.4–1000 eV electrons colliding with normal hexane and cyclohexane molecules are reported. For positron scattering, low-lying peaks at 0.8 eV for normal hexane and 1.6 eV for cyclohexane are observed. For both molecules, positron TCSs are larger than electron TCSs below 2.8 eV; for electron scattering, the main resonance peak in the TCS curve is at 7.5 eV, followed by a shoulder at about 22 eV. TCSs for normal hexane are larger than those for cyclohexane for both positrons and electrons over all the energy range. Striking similarities, more pronounced for electron impact, have been observed between *c*-hexane and benzene TCSs and are attributed to the similarity in molecular structure between these two molecules, whereby each has a hexagonal ring based on the six C atoms.

DOI: 10.1103/PhysRevA.72.042705 PACS number(s): 34.80.Bm, 34.80.Dp, 36.10.Dr

I. INTRODUCTION

Hydrocarbons play an important role in high-temperature plasmas in tokamak fusion devices in plasma processing and many other fields [1]. Electron impact cross sections are the needed parameters for modeling these processes, and the comparative study between electron and positron scattering that we carry out here offers an effective tool for better understanding electron scattering phenomena.

Our group has interests in carrying out systematic experimental investigations of total cross sections (TCSs) for positron and electron scattering from a series of alkane molecules CH_4, C_2H_6, C_3H_8, C_5H_{12}, C_6H_{14}, and C_8H_{18}, and cycloalkane molecules C_3H_6, C_5H_{10}, C_6H_{12}, and C_8H_{16} [2]. A preliminary study of positron and electron scattering TCSs for the simpler alkane molecules CH_4, C_2H_6, and C_3H_8 was carried out and reported earlier by our group [3,4]. To our knowledge, there is only one other systematic TCS study of these molecules, involving positron and electron impact, which was carried out by Floeder *et al.* [5]. However, Floeder *et al.* [5] only carried out these studies for CH_4, C_2H_6, *n*-C_3H_8, *c*-C_3H_6, *n*-C_4H_{10}, and *i*-C_4F_{10}; where *n*-, *c*-, and *i*- are abbreviations for normal, cyclo, and iso, respectively. Other studies by other groups used either the electron or positron impact [6–10]. Theoretical studies on scattering from theses molecules have been done by many groups (e.g., Ref. [9], and references therein). However, scattering studies for alkane molecules with larger numbers of carbon atoms remain scanty. Fluoroalkane (also fluorocycloalkane) molecules, in which hydrogen (H) atoms are replaced by fluorine (F) atoms, such as CF_4, C_2F_4, C_2F_6, and *c*-C_4F_8, have wide applications in the plasma processing in industry [2,11–13]. Besides our previous preliminary study [2], other studies on fluoroalkane molecules include experimental investigations of mobility, diffusion, and attachment of electrons in C_2F_4, C_2F_6, C_3F_8, and C_4F_{10} [14], and electron attachment to *n*-C_NF_{2N+2} ($N=1-6$) and *i*-C_4F_{10} [15].

In this study, positron and electron TCSs for normal (*n*)-hexane and cyclo (*c*)-hexane are comparatively investigated. Owing to the molecular structure differences between *n*-hexane and *c*-hexane, some typical features were observed in the TCSs and are discussed in this report. Without any data for differential cross sections (DCSs) for both positron and electron scattering for these individual molecules, it is impossible to determine accurately the extent of the forward scattering effect needed for correcting these TCSs. However, based on the known electron DCSs for CH_4, C_2H_6, and *n*-propane and the variation of the TCSs across the alkane (*c*-alkane) family, a speculative primitive simulation procedure has been attempted to determine DCSs for use in the correction, as a way of having some view on the extent of this effect on these TCSs. This was not attempted in the preliminary short energy range reports [2,16], wherein the former focused on the patterns in group scattering properties, and the latter dealt with the specific topics of the polarization effect and positronium formation, across the wide range of molecules studied in this laboratory.

II. EXPERIMENTAL PROCEDURE

A. Apparatus and projectiles

A ^{22}Na radioisotope with an activity of 70 μCi was used for the positron source. A set of conventional tungsten (W) ribbons, later changed to the W-mesh type, was used for the positron-beam moderator. The energy width of the positron beam is typically 2.3 eV full width at half-maximum (FWHM). On the other hand, slow electron beams with an energy width of around 1.4 eV (FWHM), for electron scattering experiments, were produced as secondary electrons emerging from the same W moderators through multiple scattering. It must be pointed out, though, that this beam energy width is different from the energy resolution of the

---

[*] Present addresses: Graduate School of Sciences, Kyushu University, Fukuoka 812-8581, Japan and Physics Department, Sophia University, Chiyoda-ku, Tokyo 102-8554, Japan.

[†] Present address: Graduate School of Sciences, Kyushu University, Fukuoka 812-8581, Japan.

1050-2947/2005/72(4)/042705(8)/$23.00

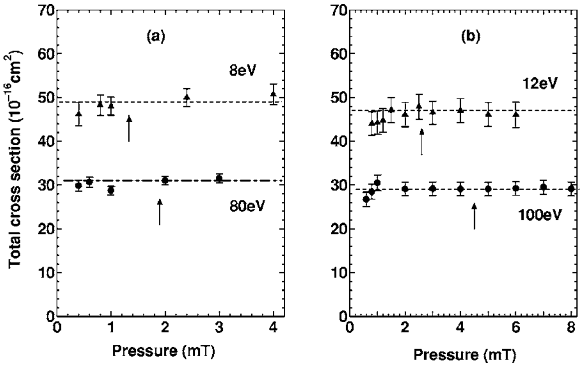

FIG. 1. TCSs plotted against gas pressure for impact energies 8.0 and 80 eV for *n*-hexane (a) and of 12.0 and 100 eV for *c*-hexane (b), respectively. The positions of the beam intensity, attenuation (I_g/I_v) of 1/3, used in for the TCS measurements are shown by the arrows. Error bars show only the statistical plus gas density errors.

retarding potential time-of-flight (RP-TOF) experimental apparatus, i.e., an average 0.24 eV below the impact energy of 4 eV, which enables discussions of structures observed even below 1 eV [17].

The apparatus for TCS measurements is a straight type TOF with a flight length of 600 mm. A retarding potential unit is included in the TOF apparatus as an energy selector for positron and electron beams. The retarding potential unit is placed in front of the beam detector (Ceratron) for eliminating the beam contribution from large energy loss inelastic scattering, and for decreasing elastically scattered and/or small energy loss such as via vibrational and rotational excitation scattered contributions with reduced axial velocities. The specimen gases for these molecules were in liquid form. The purities of the specimen liquids for *n*-hexane and *c*-hexane were 97% and 99.5%, respectively. The detailed description of the experimental procedure can be found in our previous papers [3,18]. The TCS values (Q_t) are derived from the following equation:

$$Q_t = -\frac{1}{n\ell} \ln \frac{I_g}{I_v}, \tag{1}$$

where n is gas number density in the collision cell, and ℓ is the effective length of the collision cell, which is derived from the normalization of our positron-N_2 data to the experimental TCS data of Hoffman *et al.* [19]. This process is concerned mainly with checking the pressure gauge stability. That is, the TCSs are decided relative to the experimental data of the Detroit group [19]. I_g and I_v are the beam intensities in the gas and vacuum runs, respectively. In order to ensure the independence of the TCSs on gas pressure, special TCS measurements for electron collision were performed at randomly chosen energies within the current energy range. As shown in Fig. 1, no systematic variation of TCSs with pressure is observed. This is an important aspect of measurements using a collision cell in the transmission RP-TOF setup [20], and thus needs always to be checked.

The errors in the results presented in Tables I and II are the total uncertainties computed from the equation

$$\frac{\Delta Q_t}{Q_t} = \frac{\Delta n}{n} + \frac{\Delta I}{I} + \frac{\Delta \ell}{\ell}. \tag{2}$$

This sum of all the uncertainties for positron scattering was estimated to be 6.5–13.6% for *n*-hexane and 6.7–14.7% for *c*-hexane molecules. The same sum of uncertainties for electron scattering was 5.5–6.8% for *n*-hexane and 5.5–6.4% for *c*-hexane. These sums of uncertainties are made up of contributions from the beam intensities ($\Delta I/I$), where I refers to $\ln(I_g/I_v)$ in Eq. (1) which were $<0.86\%$ ($<1.7\%$) for *n*-hexane and $<0.97\%$ ($<1.4\%$) for *c*-hexane molecules for electron (positron) scattering. The contribution from the gas density ($\Delta n/n$) was $<1\%$ for all target gas molecules and for both projectiles. That due to the determination of the effective length of the collision cell ($\Delta\ell/\ell$), was about 2% for both projectiles and all molecules. This nonquadrature addition of the errors represents the upper bound in our errors, meant to include also errors due to the forward scattering correction, which could not be explicitly quantized for the error evaluation carried out here.

B. Magnetic field and forward scattering correction

A magnetic field parallel to the flight path is applied using solenoid coils for beam transportation. The scattering beam intensity strongly depends on the magnetic field strength. Besides, the exit aperture of the collision cell is very wide, being 3 mm in radius. This means that the measured raw cross-section data ($Q_{t(measured)}$) are fairly affected by the forward scattering effect. The forward scattering effect for this apparatus can be accounted for by taking into account the forward scattering cross section (Q_f), calculated using the differential cross-secttion (DCS) data, using a simulation method described in detail elsewhere [21,22]. The synthesized DCSs for *n*-hexane were derived using the DCS data for electron scattering from CH_4 [23,24], C_2H_6 [25], and *n*-propane (C_3H_8) [26]. The synthesized DCSs are calculated by an idea based on the facts that (1) the electron-TCS data for alkane molecules vary monotonically with increasing carbon number, as can be observed in the data shown in Fig. 2; and (2) the scattering features of the electron DCS data of CH_4, C_2H_6, and C_3H_8 are not so drastically different considering the similarities of their TCS values. The intensities of the DCSs are derived using the TCS data for C_3H_8, using two assumptions: (a) the same (slight change with reference to the DCS data for CH_4 and C_2H_6) shape of DCS as C_3H_8, and (b) the intensities of the DCSs are determined with reference to the TCS data of C_3H_8 and C_6H_{14}. That is, for each energy,

$$\mathrm{DCS}_{C_6H_{14}} = \mathrm{DCS}_{C_3H_8}\mathrm{TCS}_{C_6H_{14}}/\mathrm{TCS}_{C_3H_8}. \tag{3}$$

The DCS value for C_6H_{14} due to Eq. (3) at angle zero is fairly lower than the value measured for CH_4, C_2H_6, and C_3H_8 in the plot of the extrapolation data at angle zero versus the carbon number. Taking into consideration this fact, as a small modification to the value deduced by Eq. (3), the effect of forward peaking for normal molecules was added to the DCS data for smaller angles at energies lower than 4 eV.

TABLE I. TCSs ($\times 10^{-16}$ cm^2) for positrons and electrons scattering on *n*-hexane molecules after correction for the forward scattering effect. The numbers in parentheses show the measured numerical values of the TCSs before the correction. Errors show total uncertainties derived as explained in the text.

Energy (eV)	Electron	Positron	Energy (eV)	Electron	Positron
0.2		27.2(23.8)±3.2	11	68.8(62.6)±2.3	38.5(37.2)±1.8
0.4	29.2(27.6)±1.4	31.5(28.4)±2.7	12	62.4(61.1)±2.2	39.0(37.5)±1.8
0.6	29.2(28.0)±1.2	37.6(34.8)±3.0	13	61.9(60.5)±2.3	38.7(37.3)±1.9
0.8	31.2(30.2)±1.1	42.1(39.6)±3.2	14	61.4(60.0)±2.2	37.5(36.1)±1.7
1.0	31.5(30.7)±1.1	41.1(38.8)±2.0	15	61.1(59.6)±2.2	39.0(37.5)±1.9
1.2	31.8(31.1)±1.1		16	60.6(59.1)±2.2	36.8(35.4)±1.9
1.3		37.7(35.8)±1.8	17	59.9(58.5)±2.2	37.0(35.5)±1.9
1.4	31.9(31.3)±1.1		18	60.4(58.9)±2.2	36.4(34.9)±1.8
1.6	32.3(31.8)±1.2	37.9(36.3)±1.6	19	59.2(57.7)±2.2	37.0(35.4)±1.9
1.8	33.7(33.2)±1.2		20	58.9(57.5)±2.1	37.5(36.0)±1.9
1.9		37.3(36.0)±1.6	22	58.5(57.0)±2.1	37.8(36.2)±1.7
2.0	34.4(33.9)±1.2		25	57.7(56.2)±2.1	36.0(34.4)±1.9
2.2	35.0(34.6)±1.2	36.6(35.6)±1.6	30	53.3(51.8)±2.0	37.4(35.7)±1.9
2.5	36.1(35.7)±1.3	38.6(37.5)±1.8	35	51.5(49.9)±1.9	
2.8	38.6(38.2)±1.4	36.7(35.8)±1.6	40	47.6(46.1)±1.8	36.3(34.5)±1.8
3.1	40.2(39.9)±1.5	36.1(35.2)±1.7	50	45.0(43.5)±1.7	34.9(33.1)±1.8
3.4	41.7(41.4)±1.5	35.4(34.6)±1.7	60	42.8(41.3)±1.6	33.8(32.0)±1.7
3.7	44.0(43.6)±1.7	36.2(35.4)±1.8	70	39.8(38.5)±1.5	
4.0	45.6(45.2)±1.7	37.0(36.2)±1.8	80	37.3(36.1)±1.5	31.7(30.1)±1.6
4.5	52.8(52.4)±1.9	37.2(36.2)±1.9	90	35.2(34.1)±1.4	
5.0	56.1(55.6)±2.0	38.5(37.4)±1.9	100	34.4(33.3)±1.1	30.2(28.7)±1.4
5.5	60.0(59.5)±2.3	39.6(38.4)±2.0	120	31.4(30.5)±1.1	27.8(26.5)±1.3
6.0	64.2(63.8)±2.3	40.5(39.4)±2.0	150	27.6(26.8)±0.9	24.9(23.8)±1.2
6.5	66.7(66.1)±2.4	40.5(39.2)±2.0	200	24.1(23.4)±0.8	22.0(21.0)±1.2
7.0	67.0(66.3)±2.5	40.7(39.2)±1.9	250	21.8(21.2)±0.7	19.6(18.8)±1.1
7.5	69.2(68.5)±2.5	41.4(39.7)±2.1	300	19.3(18.8)±0.6	18.2(17.5)±1.0
8.0	68.5(67.5)±2.5	41.2(39.8)±1.9	400	16.3(15.9)±0.5	16.0(15.5)±0.8
8.5	68.4(67.4)±2.6	40.7(39.3)±2.0	500	14.1(13.8)±0.5	13.4(13.0)±0.7
9.0	68.5(67.4)±2.5	40.3(38.9)±1.9	600	12.0(11.8)±0.4	11.6(11.2)±0.6
9.5	67.0(65.9)±2.5	40.4(39.0)±2.1	800	9.0(8.8)±0.3	10.2(10.0)±0.5
10	65.5(64.4)±2.4	39.7(38.4)±1.8	1000	7.1(6.8)±0.2	7.3(7.0)±0.5

The synthesized DCSs for *c*-hexane, on the other hand, have lower values at lower energies than those for *n*-propane, because *c*-hexane molecules have no dipole moment, whereas *n*-propane molecules do have (0.084 D). Theoretical DCS data for *c*-propane [9] show slightly sharper forward peaking than the experimental counterpart. *c*-hexane synthesized DCSs are derived using Eq. (3) and *c*-propane DCSs. Using the presently synthesized DCS data $[q(\theta)]$, the forward scattering cross sections (Q) are approximated using Eqs. (2)–(4) of Ref. [22]. These are then used to estimate the correct TCS value (Q_t) from the measured value ($Q_{t(measured)}$) {see Eq. (3) of Ref. [22]}. Thus, in the correction process, electron and positron TCSs are treated separately using their respective magnetic fields of 4.5 and 9 G. The forward scattering cross sections (Q_f) for electron scattering from *n*-C_6H_{14} and *c*-C_6H_{12} in the present experiment are shown together with the data for C_3H_8 in Fig. 3(a), the corresponding ratios of Q_f to TCS (Q_f/Q_t) are shown in Fig. 3(b). These results seem to be reasonable, since they do not show strange structures and considering that they are obtained using the idea of derived artificial DCSs. A similar set of results was also obtained for the positron scattering data, and the energy dependence graphs of Q_f and Q_f/Q_t are not shown here as they show the same information as Figs. 3(a) and 3(b).

III. RESULTS AND DISCUSSION

A. Positron TCSs

The TCS results are shown in Fig. 4. The numerical values are shown in Tables I and II for *n*-hexane and *c*-hexane, respectively. TCSs for *n*-hexane are greater than *c*-hexane over the whole energy. However, the difference between the two varies with energy ranges, being greatest at energies below 1.3 eV, where, for instance, it is 43% at 0.8 eV, and

TABLE II. TCSs ($\times 10^{-16}$ cm^2) for positrons and electrons scattering on *c*-hexane molecules after correction for the forward scattering effect. The numbers in parentheses show the measured numerical values of the TCSs before the correction. Errors show total uncertainties derived as explained in the text.

Energy (eV)	Electron	Positron	Energy (eV)	Electron	Positron
0.2		20.3(17.0) ± 2.6	11	53.1(51.9) ± 1.9	36.7(35.4) ± 2.0
0.4	25.0(23.6) ± 1.1	22.5(19.5) ± 2.2	12	51.1(49.9) ± 1.9	34.6(33.3) ± 1.7
0.6	24.6(23.6) ± 1.0	27.3(24.6) ± 2.5	13	50.0(48.7) ± 1.8	34.5(33.2) ± 1.8
0.8	25.9(25.1) ± 1.0	29.4(27.0) ± 2.6	14	49.4(48.1) ± 1.8	34.5(33.2) ± 1.8
1.0	27.3(26.6) ± 1.0	31.9(29.7) ± 1.8	15	49.5(48.2) ± 1.8	35.0(33.6) ± 2.0
1.2	27.8(27.2) ± 1.0		16	50.8(49.5) ± 1.9	34.3(32.9) ± 1.9
1.3		37.0(35.3) ± 1.9	17	50.1(48.8) ± 1.8	35.2(33.9) ± 2.1
1.4	28.2(27.6) ± 1.0		18	50.2(48.9) ± 1.9	34.0(32.5) ± 2.0
1.6	28.8(28.3) ± 1.0	37.4(36.0) ± 1.9	19	50.1(48.8) ± 1.8	33.6(32.1) ± 1.9
1.8	29.4(29.0) ± 1.1		20	50.2(48.9) ± 1.9	34.3(32.9) ± 1.8
1.9		37.6(36.4) ± 1.9	22	50.2(48.8) ± 1.8	34.1(32.7) ± 1.8
2.0	31.8(31.4) ± 1.2		25	49.4(48.0) ± 1.8	33.4(32.0) ± 1.9
2.2	32.4(32.0) ± 1.2	36.2(35.3) ± 1.9	30	47.7(46.2) ± 1.8	33.7(32.2) ± 1.7
2.5	33.8(33.4) ± 1.2	35.9(34.9) ± 2.0	35	46.0(44.6) ± 1.8	
2.8	35.1(34.8) ± 1.3	37.1(36.2) ± 2.0	40	44.7(43.3) ± 1.7	32.8(31.2) ± 1.7
3.1	36.3(36.0) ± 1.3	34.6(33.8) ± 1.9	50	41.1(39.8) ± 1.5	31.6(30.0) ± 1.5
3.4	37.9(37.5) ± 1.4	34.5(33.7) ± 1.9	60	39.4(38.2) ± 1.5	30.5(28.9) ± 1.4
3.7	39.1(38.8) ± 1.5	35.8(35.0) ± 2.0	70	37.0(35.9) ± 1.4	30.4(28.9) ± 1.5
4.0	43.4(43.1) ± 1.5	37.2(36.4) ± 1.9	80	34.7(33.6) ± 1.3	29.1(27.7) ± 1.5
4.5	45.2(44.8) ± 1.6	37.9(36.0) ± 1.9	90	32.5(31.5) ± 1.3	
5.0	47.0(46.5) ± 1.8	36.1(35.1) ± 2.0	100	31.2(30.3) ± 1.0	26.9(25.7) ± 1.3
5.5	51.5(51.0) ± 1.9	38.4(37.3) ± 2.2	120	28.5(27.6) ± 0.9	25.2(24.1) ± 1.3
6.0	53.7(53.2) ± 2.0	38.6(37.6) ± 2.0	150	25.5(24.8) ± 0.9	24.2(23.2) ± 1.2
6.5	55.2(54.6) ± 2.1	38.6(37.4) ± 2.0	200	22.2(21.6) ± 0.7	20.4(19.5) ± 1.0
7.0	58.9(58.3) ± 2.1	38.7(37.4) ± 1.9	250	20.1(19.5) ± 0.7	18.5(17.8) ± 0.9
7.5	59.4(58.7) ± 2.2	39.1(37.6) ± 2.0	300	18.1(17.6) ± 0.6	16.0(15.3) ± 0.9
8.0	60.3(59.6) ± 2.2	38.9(37.6) ± 1.9	400	14.9(14.5) ± 0.5	14.8(14.3) ± 0.8
8.5	59.1(58.1) ± 2.2	38.0(36.7) ± 2.0	500	13.1(12.8) ± 0.4	13.1(12.7) ± 0.8
9.0	58.5(57.5) ± 2.1	39.3(38.0) ± 2.2	600	11.7(11.5) ± 0.4	12.1(11.7) ± 0.7
9.5	57.1(56.1) ± 2.1	37.0(35.7) ± 2.0	800	9.6(9.3) ± 0.3	9.3(8.8) ± 0.5
10	55.6(54.6) ± 2.0	37.1(35.8) ± 1.8	1000	7.0(6.8) ± 0.2	7.2(6.9) ± 0.5

decreases with increasing energy above 1.6 eV until it becomes about 2% above 500 eV. Despite these magnitude differences, however, these two TCSs show close similarity in structure; i.e., the same structures at about the same energy ranges. Low-energy peaks are observed at 0.8 eV for *n*-hexane and at 1.6 eV for *c*-hexane, together with a common broad hump at 7.5 eV. In the energy range below the low-energy peak, TCSs decrease with decreasing impact energy. Above the threshold energies for positronium (Ps) formation (E_{Ps}) and ionization (E_{ion}), the increase of TCS is not remarkable at all, as expected for positron collisions [19,21]. TCSs for both molecules again show a weak peak structure in the vicinity of 20 eV, before showing a monotonically decreasing trend towards 1000 eV.

It is worth noting that, for both *n*-hexane and *c*-hexane, a small hump occurs in the positron TCS curve at about 5–9 eV. The nature and origin of this structure is not clear, but could possibly be due to positronium formation, with threshold energies of 3.33 and 3.06 eV for *n*-hexane and *c*-hexane, respectively. However, the low-energy peak features at 0.8 eV (*n*-hexane) and 1.6 eV (*c*-hexane) are not easily explainable in the limit of currently established physics. Such peak features in positron TCSs below the thresholds for Ps formation can be speculated to be either due to (i) some temporary trapping of the incoming positron by an attractive potential well, i.e., resulting in a temporary bound state of the positron-molecule system or even to some form of resonance in positron impact; or (ii) due to virtual Ps formation, whereby one of the molecular electrons joins the incoming positron temporarily to form Ps. The resulting short-range attractive interaction is similar to covalent molecular bonding. However, the net attraction can be strong enough to produce either low-lying positron-molecule virtual states or weakly bound states [28]. Further theoretical re-

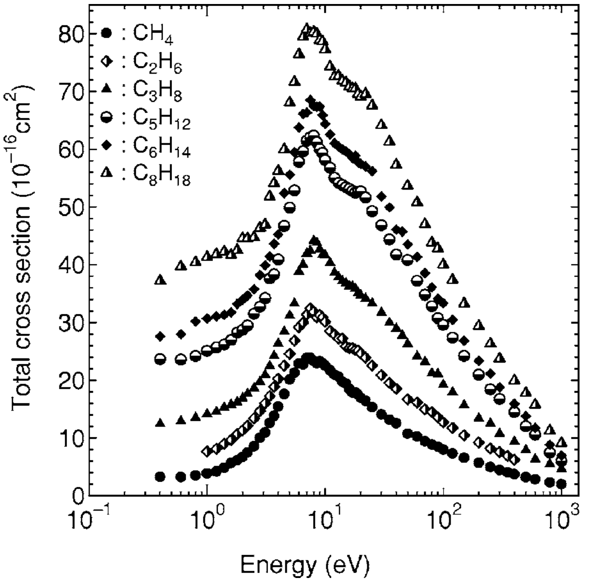

FIG. 2. Electron TCSs for alkane molecules: CH_4, C_2H_6, *n*-C_3H_8, *n*-C_5H_{12}, *n*-C_6H_{14}, and *n*-C_8H_{18}.

search is warranted to make this clear. It may also be possible that much of the physics to be learned is not from these 0.8 and 1.6 eV peaks, but from the minima that follow soon after these peaks. Such a minimum observed in positron scattering TCSs for CH_4 and C_2H_6 [3] was attributed to a weak Ramsauer minimum, in both cases, but is still to be studied for larger alkane molecules. That these two TCSs tend toward merging above 500 eV is interesting because these are structurally different molecules, and thus are expected to have different molecular sizes. However, the fact that this is observed seems to suggest that, to a high-energy positron, no significant molecular size difference exists between *n*-hexane and *c*-hexane molecules.

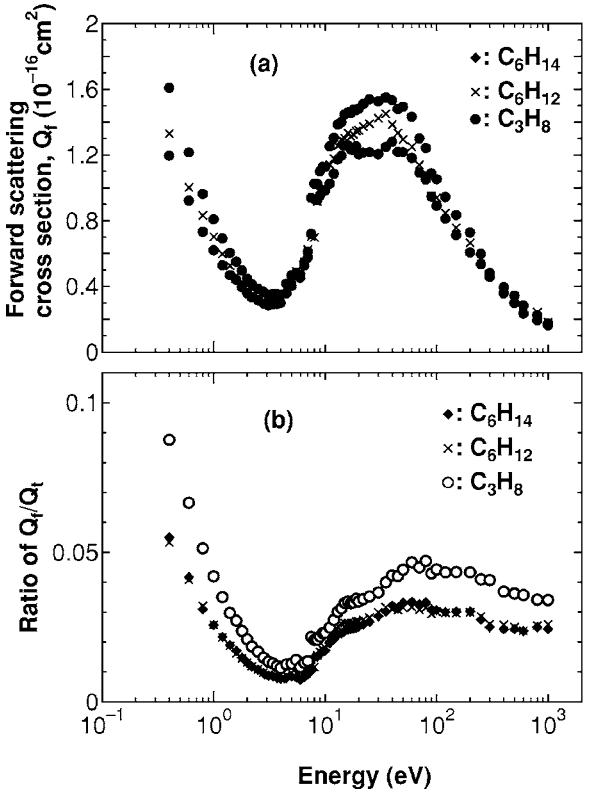

FIG. 3. (a) Electron forward scattering cross section Q_f for *n*-hexane, *c*-hexane, and *n*-propane. (b) The ratios of Q_f to TCS (Q_f/Q_t) for electron scattering from *n*-hexane, *c*-hexane, and *n*-propane.

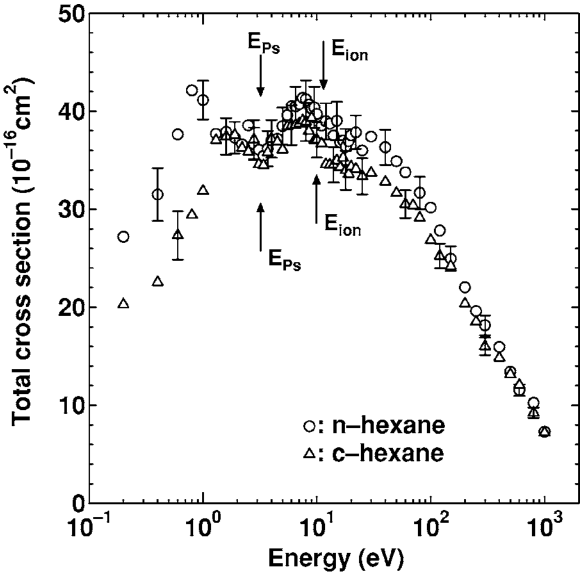

FIG. 4. TCSs for positron scattering from *n*-hexane and *c*-hexane molecules after correction for the forward scattering effect. Arrows indicate thresholds of positronium formation (E_{Ps}) and ionization (E_{ion}). Error bars show total uncertainties derived as explained in the text.

B. Electron TCSs

The TCS data for electrons colliding with *n*-hexane and *c*-hexane molecules are shown in Fig. 5. The values of TCSs for *n*-hexane are greater than *c*-hexane TCSs over the whole energy range. However, just like the positron case, this difference is greatest at low energies, being about 15–20% below 10 eV, and decreases to about 7% at 500 eV and 3% at 1000 eV. The TCS curves for both molecules do not show many resonance structures in this energy region, showing only the outstanding peak at 8 eV. However, in the energy region beyond the main peak at 8 eV, electron TCSs for both molecules show characteristic shoulders at about 15−25 eV. The 8 eV peak has been attributed to a shape resonance arising from transition into an unoccupied orbital [2]. The 15−25 eV shoulder, and another one observed by other groups at 50−60 eV, has been attributed to the admixture of the contributions from an increasing number of partial waves and the availability of unoccupied molecular orbitals at higher energies [2]. No such vivid structure exists in the corresponding positron TCS curves. Once again, just like the positron impact case above, these two TCSs tend towards "merging" in magnitude with increasing energy above 300 eV. This is an unexpected feature, for the reason that these two molecules differ significantly in molecular struc-

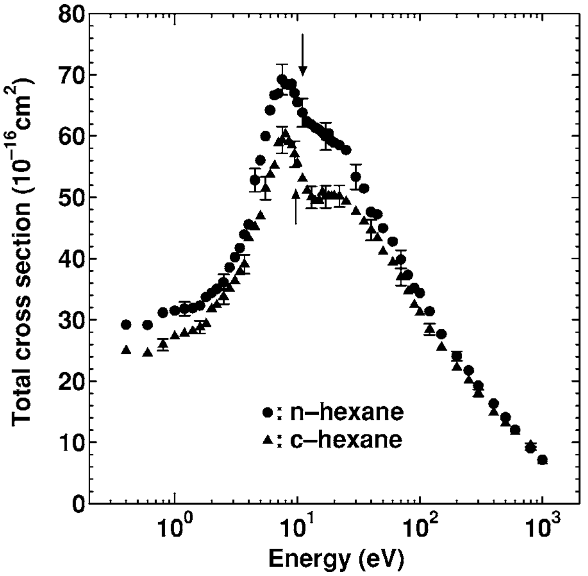

FIG. 5. TCSs for electron scattering from *n*-hexane and *c*-hexane molecules after correction for the forward scattering effect. Arrows indicate thresholds of ionization. Error bars show total uncertainties derived as explained in the text.

ture and size. However, such a tendency at these higher energies should be suggesting that these two molecules have nearly the same molecular sizes, when viewed by an oncoming high-energy electron.

C. Comparison between positron and electron TCSs

Figures 6 and 7 show positron and electron TCSs for both molecules. Merging of electron and positron TCSs is observed at energies above 200 eV. This observation should be because at these higher energies, only the first Born term dominates the scattering event. In here, the cross section varies with $(Ze^2)^2$, i.e., the square of the charge of an incoming particle, and hence, the effect of the charge difference on the cross section vanishes, leading to this convergence phenomena in the TCSs. At energies lower than 100 eV, the difference between electron and positron TCSs increases; i.e., positron TCSs are roughly constant while electron TCSs increase with decreasing impact energy. This is a clear reflection of the differences in the interaction between the electron and positron with molecules; namely, the differences due to exchange interaction and different magnitudes of static and polarization interactions. As a result, the existence of shape resonance and attachment phenomena in electron scattering results in increased structure and enhancement of TCSs compared to positron scattering. Positron TCSs at the low-energy peak region of about 1 eV, highlighted above, are larger than the electron scattering TCS data for both molecules. This reverse of TCS magnitudes has been observed for other molecules such as C_6H_6, C_2H_2, and SiH_4 [2,17]. The threshold energies for positronium formation (E_{Ps}) for these molecules are 3.33 and 3.06 eV for *n*-hexane and *c*-hexane, respectively. This means that, for both molecules, this peak around 1 eV is not due to positronium formation. Speculation leads us to make the following two possible explanations. That this peak may be due to a case whereby some modes of vibrational excitation become larger for positron impact compared to those for electron impact at these energies. Although little is known about resonances in positron scattering, the other reason for the peak could be to some type of resonance. This would be the case with an incoming positron being temporarily trapped by the polarized electron cloud of the target molecule. Similar studies of the differences between normal alkane and cycloalkane molecules will be carried out for propane, pentane, and octane molecules in coming papers.

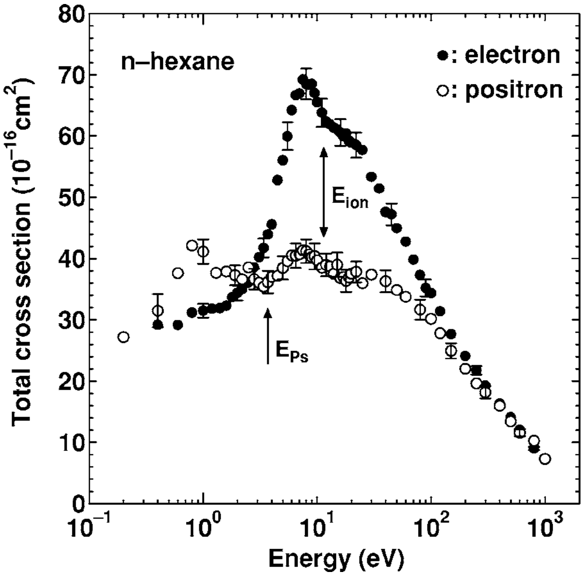

FIG. 6. Positron and electron TCSs for *n*-hexane molecules after correction for the forward scattering effect. Arrows indicate thresholds of positronium formation (E_{Ps}) and ionization (E_{ion}). Error bars show total uncertainties derived as explained in the text.

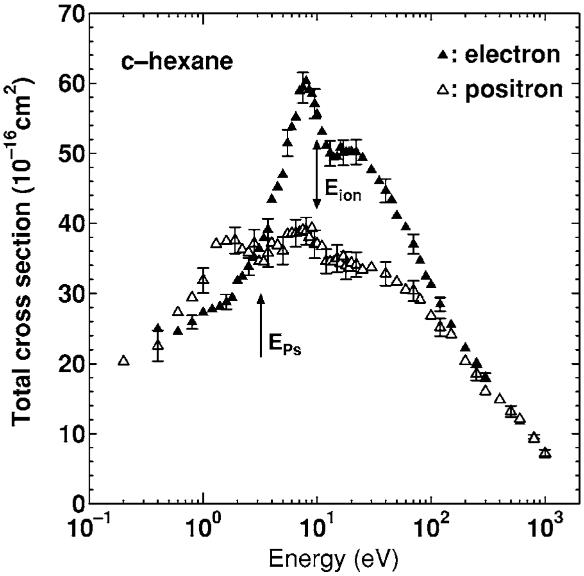

FIG. 7. Positron and electron TCSs for *c*-hexane molecules after correction for the forward scattering effect. Arrows indicate thresholds of positronium formation (E_{Ps}) and ionization (E_{ion}). Error bars show total uncertainties derived as explained in the text.

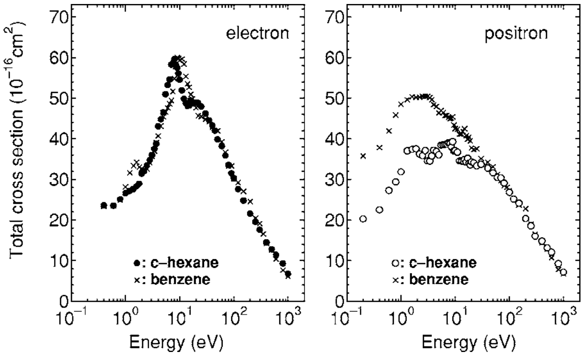

FIG. 8. Electron and positron TCSs for *c*-hexane compared with those for benzene molecules.

D. Comparison between *c*-hexane TCSs with benzene TCSs

Inspection of TCSs for various molecules studied in this laboratory led us to draw Fig. 8 which shows a comparison between the current *c*-hexane (C_6H_{12}) data and benzene (C_6H_6) TCSs. Detailed studies of the benzene TCSs, shown in Fig. 8, have already been carried out and published elsewhere [27], and will not be repeated here. At first glance, it would be quite strange to compare TCSs for these completely different molecules since the relation between the two appears to be remote. However, as described below, there are some interesting similarities between the two that may warrant some attention for careful examination. The general shape and magnitude of these two TCS results is found to be surprisingly similar, especially those for electron impact. Using the Corey-Pauling-Koltun model [30], the average diameters of these molecules were estimated and the values are shown in Table III; note the near equal magnitude in molecular diameters. Electron TCSs have magnitudes that are almost the same except for the 1.6 eV and 7–13 eV peak regions, where differences of up 20% and 9%, respectively, are observed. Both TCSs show a shoulder above the main peak in the vicinity of 10 eV, before decreasing monotonically towards 1000 eV. At energies larger than 50 eV, these two TCSs have magnitudes that are nearly equal within a few percent. The reason for this similarity, especially at these higher energies, should be refflecting more on the close similarity, Table III, in molecular structures between these two molecules. Positron TCSs however, show a lot of differences below 50 eV. Benzene TCSs are up to 60% greater than *c*-hexane TCSs below 50 eV. Although *c*-hexane TCSs show peak structures centered at about 1.6 and 7 eV, benzene TCSs are almost smoothly rising to produce the broad 0.6–20 eV peak, before decreasing beyond this peak. As in the electron case, these two TCSs become nearly equal, within experimental error, above 50 eV. As pointed earlier in the electron case, this feature should be pointing to the close similarity of the molecular structures for these two molecules. To this end, the fact that the electron impact TCSs for *c*-hexane and benzene are so similar over almost the entire energy range, whereas the corresponding positron impact TCSs are so different below 50 eV is such an interesting observation. This surely suggests that, in the collision dynamics involved with these two molecules, the electron does not “see” that much of a difference between *c*-hexane and benzene molecules, except for the two peak regions at about 1.6 eV and around 10 eV, even though the molecular structures for these two molecules are significantly different. The positron case below 50 eV is, however, different, as the molecular difference between these two molecules clearly results in different scattering dynamics as evidenced by the different TCSs. Certainly, it may be just a coincidence, but further detailed theoretical and experimental investigations on the strikingly similar shape and magnitude of the TCSs, especially for electron impact, are warranted. The obvious feature to be noted is that these two molecules each has a hexagonal ring based on the six C atoms, although the benzene ring is made up of double bonds whereas the *c*-hexane ring is single bonded. Although the number and nature of bonding of the H atoms are different, it would be reasonable to assume that the nature of bonding between the C atoms plays the more pivotal role in determining the molecular as well as electronic structures of these two molecules; hence the observed striking similarities.

TABLE III. Molecular properties for *c*-hexane and benzene molecules.

	Bond length (Å)[a]		Average molecular diameter (Å)[b]	
Bond	*c*-hexane	Benzene	*c*-hexane	Benzene
C-C	1.536	1.399	6.6	6.9
C-H	1.119	1.101		

[a] See Ref. [29].
[b] See Ref. [30].

IV. SUMMARY AND CONCLUSIONS

Normal hexane and cyclohexane TCSs for 0.2–1000 eV positron and 0.4–1000 eV electron impact energies, corrected for forward scattering effects, are presented. They fit well in the pattern of a smooth variation with change in carbon number of the TCSs of the alkane molecular family, as observed in our preliminary report. For both *n*-hexane and *c*-hexane, a small hump occurs in the positron TCS curve at about 5–9 eV, corresponding to the main peak at 8.0 eV in the electron scattering TCS curve. In the comparative study of *n*-hexane with *c*-hexane, TCSs for both electron and positron impact have been found to be very similar in energy dependence, although *n*-hexane TCSs are a few percent larger than those of *c*-hexane.

In the comparison of *c*-hexane and benzene TCSs, similarities have been observed in both electron and positron TCSs for these molecules, although the former case is more pronounced. These similarities in TCSs, especially at energies above 50 eV, have been attributed to the similarity in molecular structure between these molecules whereby each has a hexagonal ring based on the six C atoms.

ACKNOWLEDGMENTS

The authors acknowledge H. Kawate for his efforts in carrying out the forward scattering correction and Dr. A. Hamada for the measurements in the early stages. This work was partly supported by a Grant-in-Aid from the Ministry of Education, Science, Technology and Culture, Japan. C.M. is also grateful to the Japan Society for the Promotion of Science (JSPS) for financial support under Grant No. P04064.

[1] W. L. Morgan, Adv. At., Mol., Opt. Phys. **43**, 79 (2000).
[2] M. Kimura, O. Sueoka, A. Hamada, and Y. Itikawa, Adv. Chem. Phys. **111**, 537 (2000).
[3] O. Sueoka and S. Mori, J. Phys. B **19**, 4035 (1986).
[4] H. Tanaka, Y. Tachibana, M. Kitajima, O. Sueoka, H. Takaki, A. Hamada, and M. Kimura, Phys. Rev. A **59**, 2006 (1999).
[5] K. Floeder, D. Fromme, W. Raith, A. Schwab, and G. Sinapius, J. Phys. B **18**, 3347 (1985).
[6] M. Charlton, T. C. Griffith, G. R. Heyland, K. S. Lines, and G. L. Wright, J. Phys. B **13**, L757 (1980).
[7] H. Nishimura and H. Tawara, J. Phys. B **24**, L363 (1991).
[8] H. F. Winters, J. Chem. Phys. **63**, 3462 (1975); **36**, 353 (1979).
[9] R. Curik and F. A. Gianturco, J. Phys. B **35**, 717 (2002).
[10] A. Hustrulid, P. Kusch, and J. T. Tate, Phys. Rev. **54**, 1037 (1938).
[11] R. Panajotovic, M. Jelisavcic, R. Kajita, T. Tanaka, M. Kitajima, H. Cho, H. Tanaka, and S. J. Buckman, J. Chem. Phys. **121**, 4559 (2004).
[12] T. M. Miller, J. F. Friedman, and A. A. Viggiano, J. Chem. Phys. **120**, 7024 (2004).
[13] M. Jelisavic, R. Panajotovic, M. Kitajima, M. Hoshino, H. Tanaka, and S. J. Buckman, J. Chem. Phys. **121**, 5272 (2004).
[14] M. S. Naidu and A. N. Prasad, J. Phys. D **5**, 983 (1972).
[15] S. M. Spyrou, I. Saunders, and L. G. Christophorou, J. Chem. Phys. **78**, 7200 (1983).
[16] O. Sueoka, M. K. Kawada, and M. Kimura, Nucl. Instrum. Methods Phys. Res. B **171**, 96 (2000).
[17] M. Kimura, C. Makochekanwa, and O. Sueoka, J. Phys. B **37**, 1461 (2004).
[18] O. Sueoka, S. Mori, and A. Hamada, J. Phys. B **27**, 1453 (1994).
[19] K. R. Hoffman, M. S. Dababneh, Y.-F. Hsieh, W. E. Kauppila, V. Pol, J. H. Smart, and T. S. Stein, Phys. Rev. A **25**, 1393 (1982).
[20] R. E. Kennerly and R. A. Bonham, Phys. Rev. A **17**, 1844 (1978).
[21] A. Hamada and O. Sueoka, J. Phys. B **27**, 5055 (1994).
[22] O. Sueoka, C. Makochekanwa, and H. Kawate, Nucl. Instrum. Methods Phys. Res. B **192**, 206 (2002).
[23] L. Boesten and H. Tanaka, J. Phys. B **24**, 821 (1991).
[24] T. Sakae, S. Sumiyoshi, E. Murakami, Y. Matsumoto, K. Ishibashi, and A. Katase, J. Phys. B **22**, 1385 (1989).
[25] H. Tanaka, L. Boesten, D. Matsunaga, and T. Kudo, J. Phys. B **21**, 1255 (1988).
[26] L. Boesten, M. A. Dillon, H. Tanaka, and H. Sato, J. Phys. B **27**, 1845 (1994).
[27] C. Makochekanwa, O. Sueoka, and M. Kimura, Phys. Rev. A **68**, 032707-1 (2003).
[28] C. M. Surko, G. F. Gribakin, and S. J. Buckman, J. Phys. B **R57**, R126 (2005).
[29] *CRC Handbook of Chemistry and Physics*, 81st ed., edited by D. R. Lide (CRC Press, New York, 2000–2001).
[30] R. A. Harte, *Molecules in Three Dimensions: A Guide to the Construction of Models of Biologically Interesting Compounds with CPK Models* (American Society of Biological Chemists, Inc., Bethesda, MD, 1981), p. 1.